Simultaneous usage of optic and thermal hyperspectral sensors for crop water stress characterization

Luca Pipia, Fernando Pérez, Anna Tardà, Lucas Martínez, and Roman Arbiol
email: luca.pipia@icc.cat
Institut Cartogràfic de Catalunya (ICC)
Parc de Montjuïc s/n, 08038 Barcelona, Spain

ABSTRACT

Visible-Near InfraRed (VNIR) and Thermal InfraRed (TIR) simultaneous information is crucial in order to carry out a reliable description of crop water stress condition. In this paper, a study based on the hyperspectral sensors TASI and CASI, which are regularly operated by the Institut Cartogràfic de Catalunya (ICC) since 2009, is proposed. High-resolution hyperspectral data sets acquired over a vineyard in Raïmat (Spain) are employed to characterize the energy flux exchange between surface and atmosphere, and to estimate the crop daily evapotranspiration (ET_d). Finally, a relative Crop Water Stress Index (*CWSI*) is obtained under specific assumptions upon the water stress condition of reference plants within the imaged scene.

Index Terms— Evapotranspiration (ET), Crop Water Stress Index (CWSI), HypersTIR and VNIR data.

1. INTRODUCTION

Maintaining controlled levels of water stress during the growing season is essential in order to guarantee the quality of many crop productions. This is the case of grapevine cultivation, where excessive water leads to increased vegetation growth, with negative effects on grapes sugar content, pigments formation, acidity, etc. On the other hand, severe water stress induced by water shortage causes reduced assimilative activities, with negative effects on shoot growth, wood maturation and, lastly, on grapes sugar content [1]. Optimal quality parameters of grapevine cultivation can be then stimulated by maintaining slight-to-moderated water deficit, and thus controlled stress conditions. Direct measurements of crop water status are based on leaf water potential (Ψ_P) [2] or leaf conductance (LC) estimations [3]. Yet, the leaf-to-leaf variability of these quantities makes a high number of samples-per-plant necessary for reliable estimations. It follows that, despite being of great interest for research studies, these in-situ approaches become unfeasible for commercial applications.

Contrarily, an indirect estimation of crop water status is achievable through the retrieval of land surface energy fluxes from remote sensing acquisitions. The detailed knowledge of latent and sensible fluxes is of prime importance for the determination of daily evapotranspiration rate of crops, which may be directly related to crop water consumption and, hence, to crop water requirement.

Broadly speaking, the actual radiant energy available at the surface or net radiation R_n can be described as the sum of both thermodynamic and radiative contributions. According to the first factorization, it results

$$R_n = G+H+\lambda ET \quad (1)$$

where G is the Soil heat flux, H is the sensible heat flux, and λET is the latent heat flux. Namely, H accounts for rate of heat transferred to the air by convection and conduction due to temperature difference; G for the heat stored in soil and vegetation by conduction; λET for the heat rate lost through soil moisture evaporation and plant transpiration.

Alternatively, R_n may be expressed as follows

$$R_n = (1- \alpha_{bb})\tau_{bb}K_{sun}+(1- \varepsilon_{bb})\, L^{\downarrow}+ \varepsilon_{bb}\sigma T_s^4 \quad (2)$$

where α_{bb}, τ_{bb} and ε_{bb} are the broadband albedo, transmissivity and emissivity, respectively; T_s is the surface absolute temperature; K_{sun} is the solar radiation at specific latitude and time; $L^{\downarrow}$ is the atmosphere downwelling radiation; σ is the Boltzmann constant.

The daily evapotranspiration ET_d may be related to λET as follows

$$ET_d = C_{di}\, \lambda ET\, L^{-1}, \quad (3)$$

being L the latent heat of vaporization ($2.45 MJkg^{-1}$) and C_{di} the ratio between instantaneous and daily net radiation. Finally, the Crop Water Stress Index (CWSI) is given by

$$CWSI= 1- (ET_d / K_c ET_o) \quad (4)$$

where ET_o is the so-called potential evapotranspiration, which depends only on climate parameters such as air temperature, humidity, pressure and wind speed; K_c is a coefficient depending on the crop species [4].

In this paper, a study focused on the estimation of ET_d and *CWSI* over vineyards through the analysis of hyperspectral VNIR/TIR information and in-situ weather measurements is put forward. To this end, Airborne Spectrographic Imager 550 (CASI) and Thermal Airborne Spectrographic Imager (TASI) data acquired by the Institut Cartogràfic de Catalunya (ICC) in a synchronous configuration are employed. The paper is structured as follows. First, a brief description of the two sensors and the test area is provided.

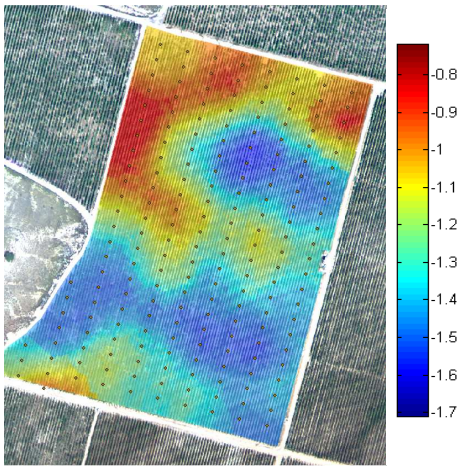

Fig.1: Kriging of Ψ_P in-situ measurements overlapped to Airborne DMC picture of the vineyard test-site in Raïmat.

Then, the estimation of the main terms in (3) and (4) is carried out to retrieve the daily evapotranspiration concerning the area of interest. In the end, a relative CWSI map is obtained using an in-scene estimation of K_c

2. SENSORS AND TEST-SITE

The Thermal Airborne Spectrographic Imager 600 (TASI-600) is a hyperspectral infrared sensor manufactured by the Canadian company ITRES©, which started being operated by the Institut Cartogràfic de Catalunya (ICC) at the end of 2009. The system works in a pushbroom configuration and provides the user with 32-band thermal infrared (TIR) hyperspectral data in the 8-11.5µm spectral window. The nominal Field-Of-View (FOV) is 40º and spreads over 600 spatial pixels. The TASI gives the opportunity to measure and retrieve information concerning skin-temperature and emissivity spectrum of the imaged scene. The TASI adds to the visible and near-infrared (VNIR) Compact Airborne Spectrographic Imager 550 (CASI) system regularly flown by the ICC since 1993. The CASI acquires data in a pushbroom configuration as the TASI, and provides up to 288-band images by focusing the VNIR radiance entering the slit from a 40.4º FOV on 550 spatial pixels. The two sensors are operated simultaneously by the MUSIC system, which was developed by ITRES to allow the user to gather hyperspectral information of up to three ITRES products at once.

The test-site selected for the study is an irrigation experimental "Tempranillo" (*Vitis vinifera*) vineyard set-up by the Institut de Recerca i Tecnologia Agroalimetrària (IRTA) in Raïmat, Spain (Lat: 41º39'58", Lon: 0º30'10"). An RGB picture acquired using ICC's DMC photogrammetric camera of the plot is shown in Fig. 1.

Different irrigation treatments are maintained within the selected field by IRTA experts for research purposes, varying from full irrigation (FI) to seasonal sustained deficit irrigation (SSDI) [5]. VNIR and TIR data were acquired on September 9, 2011, around solar noon (from 11:53 to 12:29 UTC) at two spatial resolutions. Details about the two sensors' spectral configurations and flight geometries are reported in Table 1.

FLIGHT	TASI (HIGH/LOW)	CASI (HIGH/LOW)
INTEG. TIME	14 ms	14 ms
PIXEL SIZE	0.4m/1m	0.5m/1m
HEIGHT (ft)	1000/2460	1000/2460
# BANDS	32	5
SPECTRAL WINDOW	[8µm:11.5 µm]	Ch:452,542,633, 724,816 [nm]

Table 1: Flight parameters and sensors' spectral configuration of the measuring campaign in Raïmat.

In-situ LWP measurements were taken by IRTA simultaneously to the image capture. The spatial distribution of the ground-truth points is depicted in Fig.1. A Kriging interpolation was applied to obtain a 2D distribution of Ψ_P.

3. HYPESPECTRAL DATA PROCESSING

Hyperspectral TIR data provided by TASI were processed to retrieve a reliable description of the surface absolute temperature T_s and broadband emissivity ε_{BB} at pixel level. The radiative transfer equation applied to the TIR region is

$$L(\theta)_{s,i}=[\varepsilon_i B_i(T_s)+(1-\varepsilon_i)L(\theta)_i^{\downarrow}]\tau_i(\theta) + L_i(\theta)^{\uparrow} \quad [i=1,..N] \quad (5)$$

where θ is the observation angle, i denotes the spectral channel, τ is ith-channel total transmissivity, $L_i(\theta)^{\uparrow}$ and $L_i(\theta)^{\downarrow}$ are the up and downwelling radiances, respectively.

In order to separate T_s and ε_i, which are coupled in (1), a processing chain developed at ICC was applied [6]. After the radiometric calibration step, which converted DNs into radiance information, the observation geometry was calculated for each pixel of the image. These parameters were passed to the ModTRAN5.0 SW for the estimation of the atmospheric thermal parameters. Since no simultaneous radiosounding measurement was at disposal, the vertical profiles for air temperature, humidity and pressure provided by the National Centres for Environmental Prediction (NCEP) [7] at the vineyard coordinates were employed.

Finally, the separation step was carried out using the Temperature and Emissivity Separation (TES) technique proposed in [8]. Generally, the method uses land-leaving hyperspectral radiance and a semi-empirical relationship between the minimum emissivity ε_{min} and the maximum-minimum spectral difference MMD. In order to apply this technique to TASI data, a new semi-empirical model tailored to TASI spectral properties was developed using the Aster2.0 spectral library information. Broadband emissivity ε_{BB} was finally calculated by averaging the emissivity vector retrieved at pixel level. The temperature map obtained for the vineyard area is shown is Fig. 2.

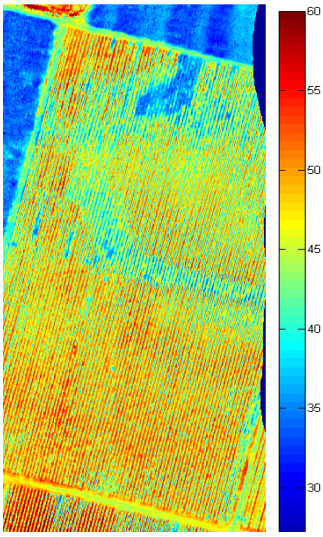

Fig.2: Temperature map [ºC] of the vineyard in Raïmat.

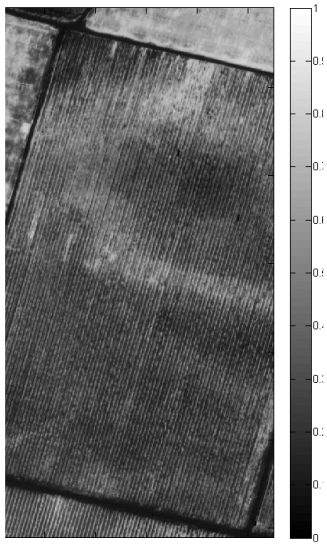

Fig.3: *NDVI* map of the vineyard in Raïmat.

The atmospheric correction of the hyperspectral CASI radiance imagery was performed with an atmospheric correction system [9] developed at ICC. It basically consists of a physical model of the radiative transfer with 6S method simulations adapted to the characteristics of the CASI airborne sensor. Standard water vapor content, aerosols profile and aerosols total load were used. At the end of the process, a reflectivity vector for each pixel of the imaged area was obtained. Finally, α_{bb} was calculated as follows [10]:

$$\alpha_{bb} = 0.5(\rho_{RED}+\rho_{NIR}) \quad (7)$$

where ρ_{RED} and ρ_{RED} represent the reflectivity information retrieved @633nm for RED (Band 3) and @816nm for NIR (Band 5). The Normalized Difference Index Vegetation (NDVI) calculated using CASI-based RED and NIR reflectivity information is shown in Fig.3.

4. ENERGY BALANCE SOLUTION

The processing of TASI and CASI simultaneous data provided the terms α_{bb}, ε_{bb}, and T_s. In order to calculate R_n, a few additional parameters, which are related to climate conditions, had to be estimated. Being clear-sky assumption fulfilled the day Raïmat data sets were acquired, the standard Mid-Latitude Summer atmospheric profile of ModTRAN 5.0 was employed to calculate both τ_{bb} and $L^{\downarrow}$; K_{sun} was obtained using the solar irradiance model in [4], which takes into account the day of the year and the time of the day when measurements were gathered. In order to estimate λET, eq. (1) may be rearranged as proposed in [11]:

$$\lambda ET = R_n - G - H = R_n \Lambda(1-\Gamma) \quad (8)$$

where Λ is the evaporative fraction and Γ is the soil heat/net radiation flux density ratio. Λ ranges in [0,1] and describes

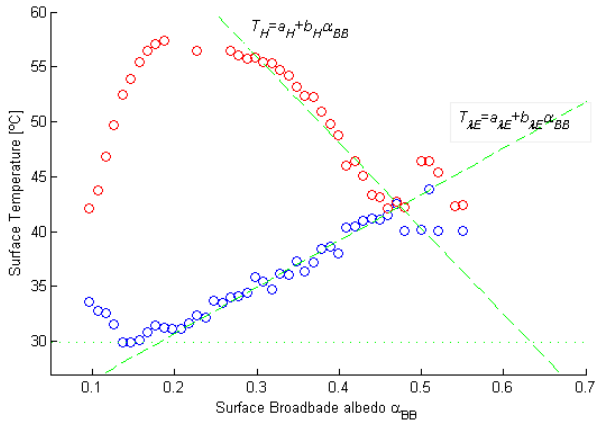

Fig.4: Lines delimiting upper and lower boundaries of α_{bb} vs *Ts* 2D-distribution estimated over the vineyard for Λ retrieval.

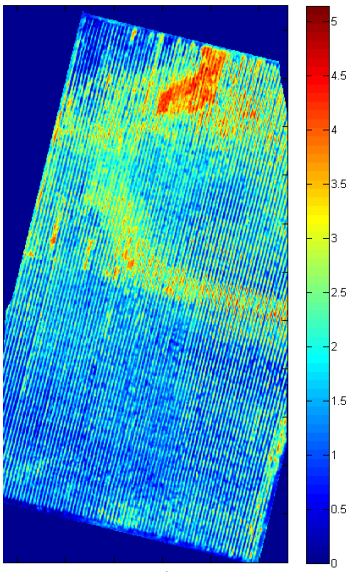

Fig.5: ET_d map [mmday^{-1}] of the vineyard in Raïmat.

the capability of each pixel to lose heat through soil moisture evaporation or plant transpiration. It was calculated as

$$\Lambda = (a_H+b_H\,\alpha_{bb} - T_s)/(a_H-a_{\lambda E}+([b_H-b_{\lambda E}]\alpha_{bb}), \quad (9)$$

where the coefficients a and b were estimated from the α_{bb} versus T_s distribution as explained in [11] and sketched in Fig.4; a mask delimiting the perimeter of the vineyard was employed to filter out pixels belonging to other types of coverage. Concerning the term Γ, it may be calculated using the empirical relationship found in [11]

$$\Gamma = T_s[ºC](0.32\alpha_{bb} + 0.62\alpha_{bb}^2)(1-0.978NDVI^2)\alpha_{bb}^{-1}. \quad (10)$$

In order to obtain ET_d from λET, eq. (3) was applied. The coefficient C_{di} was calculated using the ratio between the instantaneous and daily solar net radiation measured by the meteorological station of Segrià (Raïmat), located at about 5 km from the area of interest, under the assumption of daily ground heat flux close to zero [4]. The result is shown in Fig. 5.

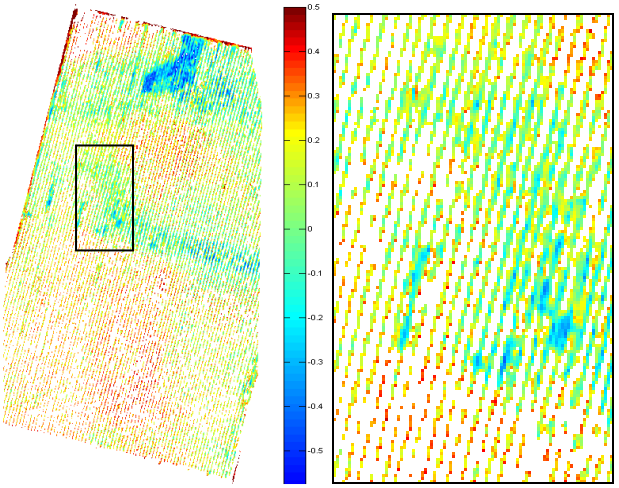

Fig. 6: $CWSI_{rel}$ distribution over the area of interest in Raïmat.

The last step of the processing chain is the retrieval of CWSI using eq. (4). The term ET_0 was obtained by the Penman-Monteith equation in [4] using air temperature, relative humidity, and wind speed measurements at 2m height information taken in Segrià. The value of ET_0 retrieved for Raïmat area on September 9, 2011, was around 4.3 mm day^{-1}.

For the estimation of water stress index, two possible solutions were available. The first one was the use of a tabulated value for K_c in (4). Yet, it must be remarked that this value often does not account for the specific status of the plants to be characterized. Thus, a relative CWSI was preferred. Denoting with $CWSI_{REF}$ a reference value of the water stress index corresponding to a specific area of the monitored crop, a relative CWSI map of the whole area of interest can be obtained as follows:

$$CWSI_{rel} = 1 - (ET_d / K_{cREF} ET_o) \quad (11)$$

where

$$K_{cREF} = ET_o\,(1 - CWSI_{REF})\,ET_{d,REF}. \quad (12)$$

This approach makes it possible to carry out a description of the water stress over an area of interest taking into account the specificity of the plants under observation. Note that the *a priori* information required to apply (11) may correspond to plants ranging from no-stress to fully-stress conditions, as far as they represent a reference status for the retrieval of useful information.

The red area in the upper part of the Fig. 5 defines a region of the vineyard subject to very low water deficit. Yet, the corresponding high values of NDVI (Fig.3) are due to the dense low vegetation covering the soil around grapevine trunks. For this reason, the reference plants were selected along the diagonal low-temperature zone defining the location of irrigation pipeline: it was assumed $CWSI_{REF}$=0, which provided K_{cREF}=0.75. The CWSI map obtained over the vineyard in Raïmat is shown in Fig. 6, where a zoom on a part of the lot is also provided. Positive or negative values of $CWSI_{rel}$ correspond to higher or lower water stress conditions with respect to the reference value. The area characterized by values close to -0.5 correspond to dense low vegetation, which showed properties close to Penman-Monteith reference crop, hence with higher transpiration rate than grapevines. A NDVI-Temperature mask was applied to filter out soil contributions.

5. CONCLUSIONS

In this paper, a robust processing based on hyperspectral VNIR and TIR data solving the surface energy balance equation and retrieving the crop daily evapotranspiration ET_d has been put forward. For the study, simultaneous CASI and TASI data acquired by the Institut Cartogràfic de Catalunya (ICC) in Raïmat (Spain) have been employed. Additionally, the possibility of obtaining a relative description of crop water stress based on in-scene reference pixels selection has been provided. A quantitative validation of the method based on empirical relationships between leaf water potential Ψ_P and absolute values of CWSI is now required and will represent the focus of future studies.

6. REFERENCES

[1] M.Möller, et al., "Use of thermal and visible imagery for estimating crop awater status of irrigated grapevine," *Journal of Exp. Botany*, Vol. 58, No. 4, pp. 827-838m 2007.

[2] F. Tardieu and T. Simonneau, "Variability among species of stomatal control under fluctuating soil water status and evaporative demand: modelling isohydric and anisohydric behaviours," *Journal of Exp. Botany*, Vol. 49, pp. 419–432.

[3] H.G. Jones, "Irrigation scheduling: advantages and pitfalls of plant-based methods," *Journal of Exp. Botany*, Vol. 55, No. 407, pp. 2427–2436.

[4] R.G. Allen et al., "Crop Evapotranspiration- Guidelines dor computing crop water requirements," FAO Irrigation and drainage paper 56, Rome, 1998.

[5] J.Marsal and A. Utset, "Vineyard Full Irrigation Requirements Under Climate Change Scenarios for EbroValley – Spain," *Acta Horticulturae*, Vol. 803 (2007)

[6] L. Pipia et al., "Potentials of the Thermal Airborne Spectrographic Imager for Environmental Studies", *9th Int. Geomatic Week*, 15-17 March 2011, Barcelona, Spain.

[7] J.A.Barsi, J.R.Barker, J.L.Schott, "An Atmospheric Correction Parameter Calculator for a Single Thermal Band Earth-Sensing Instrument," *IGARSS03*, 21-25 July 2003, Toulouse, France.

[8] A.Gillespie et al. "Temperature and Emissivity Separation from Advanced Spaceborne Thermal Emission and Reflection Radiometer (ASTER) images", *TGRS*, Vol. 35, No. 4, pp.1113-1126.

[9] L. Martínez et al., "Atmospheric correction algorithm applied to CASI multi-height hyperspectral imagery," RAQRS II, 25-29 September 2006, València, Spain.

[10] R.W. Saunders, "The determination of broad land surface albedo from AVHRR visible and near infrared radiance," *Int. J. of Rem. Sens*., Vol .11, pp- 49-67.

[11] G.J. Roerink, et al., "S-SEBI: A Simple Remote Sensing Algorithm to Estimate the Surface Energy Balance," *Phys. Chem. Earth*, Vol. 25, No. 2, pp 147-157, 2000.